Temperatureenhanced electron detachment from C6F6 − negative ions

P. G. Datskos, L. G. Christophorou, and J. G. Carter

Citation: The Journal of Chemical Physics **98**, 7875 (1993); doi: 10.1063/1.464595
View online: http://dx.doi.org/10.1063/1.464595
View Table of Contents: http://scitation.aip.org/content/aip/journal/jcp/98/10?ver=pdfcov
Published by the AIP Publishing

Temperature-enhanced electron detachment from $C_6F_6^-$ negative ions

P. G. Datskos,[a] L. G. Christophorou,[a] and J. G. Carter
Atomic, Molecular, and High Voltage Physics Group, Health and Safety Research Division, Oak Ridge National Laboratory, Oak Ridge, Tennessee 37831-6122

(Received 23 December 1992; accepted 8 February 1993)

A method is described whereby photoelectrons generated by a short laser pulse at the cathode of a parallel-plate electrode arrangement are depleted by attachment to C_6F_6 molecules mixed with N_2 in the interelectrode space as they drift to the anode under an externally applied electric field. The contribution of the initially produced (prompt) and the delayed (autodetached from $C_6F_6^-$) electrons to the induced signal in the detector circuit is recorded as a function of time following the laser pulse and also as a function of gas number density, applied electric field, and gas temperature, T. Increases in T from ambient to 575 K enhance dramatically the autodetachment frequency, τ_d^{-1}, for $C_6F_6^-$. This heat-activated autodetachment correlates with the increase in the internal energy of the anion and has an activation energy of 0.477 eV. Electron attachment producing $C_6F_6^-$ initially increases slightly with increasing T below 500 K and subsequently decreases with further increases in T.

I. INTRODUCTION

Earlier studies[1–5] have shown that hexafluorobenzene (C_6F_6) captures electrons through both (low lying) nondissociative and (higher lying) dissociative negative ion states. The negative ion resonances (NIRs) observed in C_6F_6 can generally be understood[1,4,5] by considering the capture of the incoming electron into one of the three empty π-orbitals π_4, π_5, and π_6. Electron transmission experiments[1] demonstrated the existence of three NIRs. For the first two degenerate NIRs associated with the π_4, π_5 orbitals, a vertical attachment energy (VAE) of $\sim$0.42 eV was reported and for the third NIR associated with the π_6 orbital the reported value of the VAE is $\sim$4.5 eV. Literature values for the electron affinity (EA) of C_6F_6 vary from 0.52 to more than 1.8 eV.[6–15] Since the dissociation energy $D(C_6F_5\text{–}F)$ is $\sim$3.45 eV (Ref. 16) and the EA of the F atom and the C_6F_5 radical are, respectively, 3.4 and 2.7 eV (see Ref. 15) dissociative electron attachment leading to F^- and especially $C_6F_5^-$ is not expected at thermal energies. Hence the negative ions formed at thermal energies are expected to be due to $C_6F_6^-$ parent anions. Indeed electron beam studies[2,3] have shown the formation of F^- and $C_6F_5^-$ at $\sim$4.0 and $\sim$4.5 eV, respectively, and the formation of the parent anion $C_6F_6^-$ at low energies and with the parent anion's intensity rising towards thermal electron energies; electron beam studies using a time of flight mass spectrometer measured[3] the autodetachment lifetime of $C_6F_6^-$* and found it to be $\sim$12 μs at room temperature. Increases in the energy of the captured electron leads to smaller autodetachment lifetimes[17,18] for $C_6F_6^-$*.

Room temperature electron swarm studies[5,19] found that electron attachment to C_6F_6 was very strong at mean electron energies, $\langle\epsilon\rangle$ below 1.5 eV. The electron attachment cross section deduced[5] from the swarm measurements possesses two peaks; one at $\sim$0.0 eV and another at $\sim$0.73 eV. The process responsible for the thermal energy peak was associated with electron capture into the degenerate π_4 and π_5 molecular orbitals, and that at $\sim$0.73 eV with the π_6 NIR. Electron swarm studies[20–24] of the attachment of *thermal* electrons to C_6F_6 at temperatures above ambient have reported that the rate constant for thermal electron attachment decreases profoundly with increasing T; electron swarm studies at mean electron energies from thermal to $\sim$1 eV showed[23] decreases in the attachment rate constant k_a by more than two orders of magnitude as T was raised from 450 to 600 K. It was suggested that the observed decreases in $k_a(T)$ could be due to changes in the capture process[23,24] forming $C_6F_6^-$* and/or due to electron detachment from the parent anion.[22] A more recent study[25] at thermal electron energies reported that the decrease in k_a with increasing T is indeed due to electron detachment from stabilized $C_6F_6^-$ and measured the electron detachment frequency in the temperature range 300–350 K. This was accomplished by monitoring the temporal profile of the $C_6F_6^-$ anions at ms times following the formation of $C_6F_6^-$*. In the present study we determined the electron attachment rate constant and the electron detachment frequency by recording the transient electron current due to prompt and delayed (detached) electrons.

In the present study we measured the electron attachment rate constant for the formation of $C_6F_6^-$ and the electron detachment frequency for $C_6F_6^-$ as a function of T (300–575 K) and $\langle\epsilon\rangle$ ($\sim$0.187 to $\sim$1.0 eV). This we accomplished by recording the transient electron current due to prompt and delayed (detached) electrons within microsecond and submicrosecond times following the injection of the initial electrons into the gas from the cathode using a fast laser pulse (see Sec. II). These electrons drift to the anode under an externally applied uniform electric field. The interelectrode space was filled with minute amounts of C_6F_6 in a buffer gas of N_2. For the N_2 number densities used (1.61×10^{19} to 9.66×10^{19} molecules cm^{-3}) the initially produced (prompt) electrons attain quickly

[a]Also at The Department of Physics and Astronomy, The University of Tennessee, Knoxville, Tennessee 37996-1200.

 0021-9606/93/107875-08$06.00

(through collisions with the gas molecules) an equilibrium energy distribution $f(\epsilon,\langle\epsilon\rangle,T)$ which is well characterized under our experimental conditions.[26] At each value of the density, N, reduced electric field, E/N, employed the $f(\epsilon,\langle\epsilon\rangle,T)$ is calculated[27] and hence $\langle\epsilon\rangle(E/N,T)$ is determined and therefore the measured attachment rate constant and electron detachment frequency can be obtained as a function of $\langle\epsilon\rangle$ and T. The attachment and detachment processes envisioned are

$$e+C_6F_6 \xrightarrow{k_c} C_6F_6^{-*} \xrightarrow{N_2} C_6F_6^-, \tag{1}$$

$$C_6F_6^- \xrightarrow{\tau_d^{-1}} C_6F_6+e, \tag{2}$$

namely, electrons are captured by the C_6F_6 molecules with a rate constant k_c forming transient negative ions $C_6F_6^{-*}$ which are subsequently stabilized via collisions with (primarily) N_2 molecules forming $C_6F_6^-$. Electrons are thermally detached from $C_6F_6^-$ [reaction (2)] with an autodetachment frequency τ_d^{-1}. In this paper we studied reactions (1) and (2) as a function of T and $\langle\epsilon\rangle$ and concluded that the reduction in stable parent anion formation at elevated T is principally due to the large increase in the autodetachment from $C_6F_6^-$ with increasing T.

II. EXPERIMENTAL TECHNIQUE AND MEASUREMENTS

The experimental set up is shown schematically in Fig. 1. The cell used consists of a six way stainless steel cube

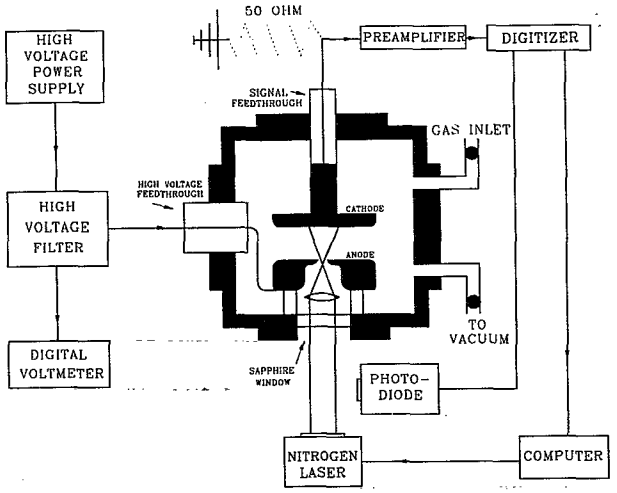

FIG. 1. Schematic diagram of the experimental set up.

with one sapphire window to allow the laser light to enter the cell. The two parallel stainless steel electrodes were circular disks of 3.81 cm in diameter and were held a distance of 0.4183 cm apart. The laser employed to produce the photoelectrons from the cathode was a Laser Photonics model LN 1000 nitrogen laser. The laser wavelength was 337.1 nm and the laser pulse duration (FWHM) was 6×10^{-10} s. The laser light strikes the cathode after going through a 0.1 cm diam hole in the anode electrode. A

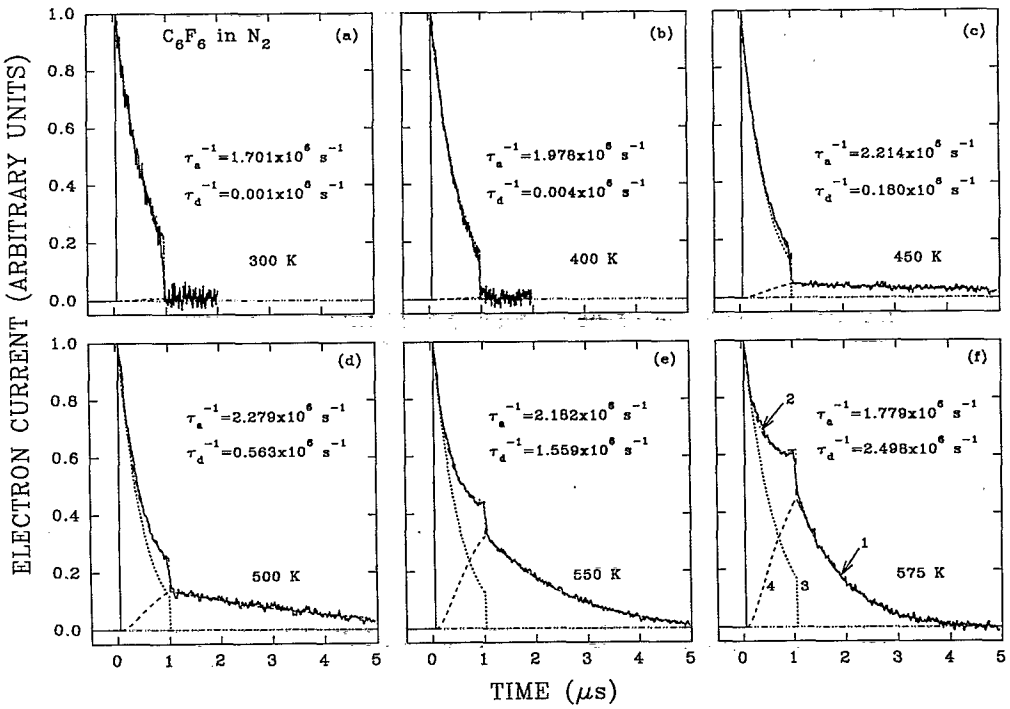

FIG. 2. Electron current waveforms for C_6F_6 at $T=300$, 400, 450, 500, 550, and 575 K. All waveforms are for $E/N=1.087\times10^{-17}$ V cm^2, $N_T=9.66\times10^{19}$ molecules cm^{-3}, $N_a=5.64\times10^{13}$ molecules cm^{-3}, and $d=0.4183$ cm (see the text). In the figure the solid curves (-) [curve 1 in (f)] are the experimentally measured total electron currents as a function of time; the dash–dot (-·-) curves [curve 2 in (f)] are the calculated electron current waveforms for the τ_a^{-1} and τ_d^{-1} values obtained from the fitting of the model (see the text) to curves 1; the dotted (···) curves [curve 3 in (f)] represent the contribution to the total electron current of the initial (prompt) electron swarm when only electron attachment occurs, and the broken (---) curves [curve 4 in (f)] represent the contribution to the total electron current from the autodetached electrons.

converging lens is employed to pass the laser beam through the hole to the cathode; the illuminated area on the cathode is ~ 1.5 cm^2.

A uniform electric field was applied to drift the electrons to the anode. The motion of the electrons (and the ions formed) in the interelectrode gap was detected and recorded with a Tektronix 7912 AD digitizer through a 50 Ω resistor to ground. The induced signal in the detection circuit is proportional to the electron and ion currents in the gap which themselves depend on the electron and ion drift velocities and the initial electron number density. However, the contribution to the current in the time scales of interest in this study is solely from the electrons and not from the negative ions.

The experiments were performed using N_2 as the buffer gas which was of Matheson ultrahigh purity (99.999%). Before use, the N_2 gas was cooled to liquid nitrogen temperature to freeze out any condensible impurities. The C_6F_6 sample was obtained from Aldrich Chemical Company with a stated purity of 99.9%. The C_6F_6 sample was subjected to several vacuum distillation cycles prior to the measurements in order to remove any air from the sample. The total gas number density, N_T, was varied from 1.61 to 9.66×10^{19} molecules cm^{-3}, and the attaching gas number density, N_a, was varied from 1.93×10^{13} to 38.64×10^{13} molecules cm^{-3}. A heating jacket was used to maintain the desired temperature which in turn was measured with two thermocouples in the cell.

The time and space evolution of the electron swarm when both electron attachment and detachment (but no ionization) processes are present can be described,[28–31] by

$$\frac{\partial\rho_e(x,t)}{\partial t}+w_e\frac{\partial\rho_e(x,t)}{\partial x}=-\frac{1}{\tau_a}\rho_e(x,t)+\frac{1}{\tau_d}\rho_i(x,t), \quad (3)$$

$$\frac{\partial\rho_i(x,t)}{\partial t}+w_i\frac{\partial\rho_i(x,t)}{\partial x}=\frac{1}{\tau_a}\rho_e(x,t)-\frac{1}{\tau_d}\rho_i(x,t), \quad (4)$$

where $\rho_e(x,t)$ and $\rho_i(x,t)$ is the number density of the electrons and negative ions, respectively, w_e and w_i are their respective drift velocities, and τ_a^{-1} and τ_d^{-1} are, respectively, the electron attachment and detachment frequencies. The solution to Eqs. (3) and (4) when the initial electron swarm is produced by a short duration laser pulse, i.e., for initial conditions $\rho_e(x,0)=n_0\delta(x)$ and $\rho_i(x,0)=0$ is given by[28–31]

$$\rho_e(x,t)=\frac{n_0}{w_e-w_i}\exp\left[-\frac{1}{\tau_a}\left(\frac{x-w_it}{w_e-w_i}\right)+\frac{1}{\tau_d}\left(\frac{x-w_et}{w_e-w_i}\right)\right]\times\left[\delta\left(\frac{w_et-x}{w_e-w_i}\right)+\sqrt{\frac{1}{\tau_a\tau_d}\frac{x-w_it}{w_et-x}}\times I_1\left[\frac{2}{(w_e-w_i)}\sqrt{\frac{1}{\tau_a\tau_d}(w_et-x)(x-w_it)}\right]\right], \quad (5)$$

$$\rho_i(x,t)=\frac{n_0}{w_e-w_i}\frac{1}{\tau_a}\exp\left[-\frac{1}{\tau_a}\left(\frac{x-w_it}{w_e-w_i}\right)+\frac{1}{\tau_d}\left(\frac{x-w_et}{w_e-w_i}\right)\right]\times I_0\left[\frac{2}{(w_e-w_i)}\sqrt{\frac{1}{\tau_a\tau_d}(w_et-x)(x-w_it)}\right], \quad (6)$$

where n_0 is the initial electron number density, $\delta[(w_et-x)/(w_e-w_i)]$ is the delta function and I_n is the nth order modified Bessel function.

The electron and negative ion currents can be determined from

$$i_e(t)=\frac{ew_e}{d}\int_{w_it}^{\min[w_et,d]}\rho_e(x,t)dx, \quad (7)$$

$$i_i(t)=\frac{ew_i}{d}\int_{w_it}^{\min[w_et,d]}\rho_i(x,t)dx, \quad (8)$$

where d is the interelectrode gap.

We can define the electron attachment and detachment rate constants as

$$k_a\left(=\frac{\eta w_e}{N_a}\right)=(\tau_aN_a)^{-1}, \quad k_d=\tau_d^{-1}, \quad (9)$$

where η is the electron attachment coefficient defined[29,30] as the mean number of attachment collisions for one electron traveling 1 unit length along the direction of the electric field. By a nonlinear least squares fit of Eq. (7) to the experimental waveforms, $\tau_a^{-1}(\langle\epsilon\rangle,T)$ and $\tau_d^{-1}(\langle\epsilon\rangle,T)$ can be determined and from these the electron attachment rate constant $k_a(\langle\epsilon\rangle,T)$ and the autodetachment frequency $\tau_d^{-1}(\langle\epsilon\rangle,T)$. Examples of typical experimental waveforms are shown in Fig. 2 for $T=300$, 400, 450, 500, 550, and 575 K. The evolution of the autodetachment process for C_6F_6 as T is increased can be viewed in Fig. 2. In this figure the solid curves are the experimental waveforms for $\langle\epsilon\rangle\approx0.38$ eV ($E/N=1.087\times10^{-17}$ V cm^2), $N_T=9.66\times10^{19}$ molecules cm^{-3}, $N_a=5.64\times10^{13}$ molecules cm^{-3} and for a drift gap, d, of 0.4183 cm. The dotted curves represent the contribution to the total electron current when no autodetachment occurs. The difference between the total electron current (solid curves) and the dotted curves represents the contribution of the autodetached ("delayed") electrons (dashed curves). As T is increased this contribution becomes increasingly more significant and the parent anions decay faster.

III. RESULTS AND DISCUSSION

A. Electron attachment rate constant $k_a(\langle\epsilon\rangle,T)$ as a function of $\langle\epsilon\rangle$ and T

As mentioned in the Introduction the electron energy distribution functions $f(\epsilon,\langle\epsilon\rangle,T)$ for N_2 are known under our experimental conditions and thus at each value of E/N and T employed, the mean electron energy $\langle\epsilon\rangle(E/N,T)$ can be determined. For a number of $\langle\epsilon\rangle$ values we determined (from waveforms such as in Fig. 2) the $\tau_a^{-1}(\langle\epsilon\rangle,T)$ and $\tau_d^{-1}(\langle\epsilon\rangle,T)$ simultaneously via a nonlinear least squares fit procedure. Typical fits are shown in Fig. 2 for electron current waveforms for C_6F_6 at $T=300$, 400, 450,

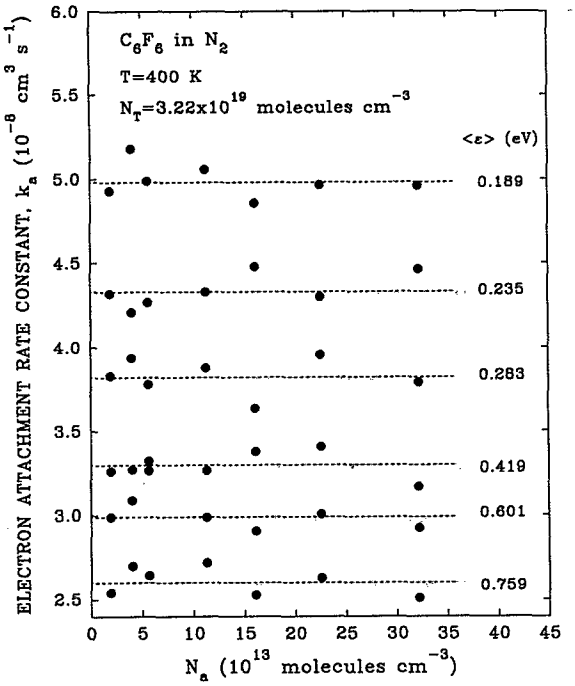

FIG. 3. Electron attachment rate constant k_a for C_6F_6 as a function of the attaching gas number density N_a for several values of the mean electron energy $\langle\epsilon\rangle$ and fixed values of T (400 K) and N_T (3.22×10^{19} molecules cm^{-3}).

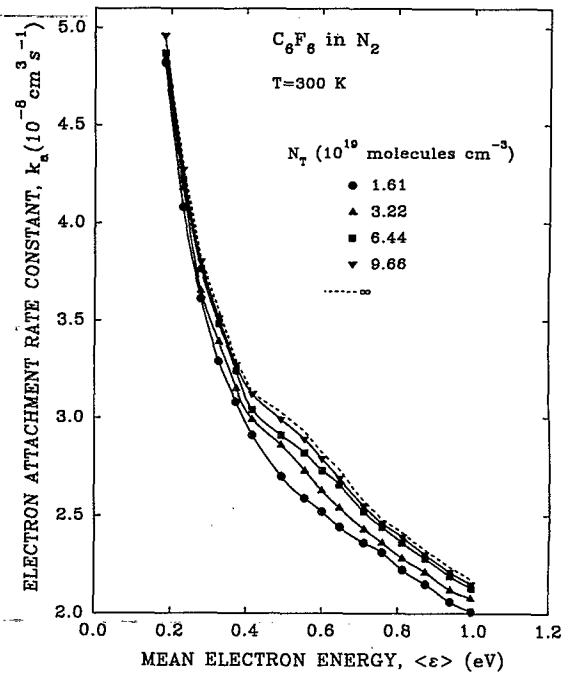

FIG. 4. Electron attachment rate constant k_a (for $N_a\to0$) for C_6F_6 as a function of mean electron energy, $\langle\epsilon\rangle$, and the total gas number density, N_T, at $T=300$ K. The broken curve is the electron attachment rate constant for $N_T\to\infty$.

500, 550, and 575 K. In the figure the solid curves (—) [curve 1 in Fig. 2(f)] are the experimentally measured total electron currents as a function of time; the dash–dot (-·-) curves [curve 2 in Fig. 2(f)] are the calculated electron current waveforms for the τ_a^{-1} and τ_d^{-1} values obtained from the fitting of the model to curves 1; the dotted (···) curves [curve 3 in Fig. 2(f)] represent the contribution to the total electron current of the initial electron swarm when only electron attachment occurs, and the broken (---) curves [curve 4 in Fig. 2(f)] represent the contribution to the total electron current from the autodetached electrons. Once $\tau_a^{-1}(\langle\epsilon\rangle,T)$ was determined this way, the total electron attachment rate constant $k_a(\langle\epsilon\rangle,T)$ for C_6F_6 at 300, 400, 450, 500, 550, and 575 K was calculated through Eq. (9). The $k_a(\langle\epsilon\rangle,T)$ was found to be independent of the attaching gas number density N_a at all T (see Fig. 3) but exhibited a small increase with increasing total gas number density, N_T (Fig. 4). The increase in $k_a(\langle\epsilon\rangle,T)$ with increasing N_T is due to the collisional stabilization of the transient $C_6F_6^{-*}$ anions. From data such as in Fig. 4 the values of $\lim_{N_T\to\infty} k_a(\langle\epsilon\rangle,T)$ were determined (by plotting $1/k_a$ as a function of $1/N_T$ and extrapolating $1/N_T$ to 0) at 300, 400, 450, 500, 550, and 575 K. These values of $k_a(\langle\epsilon\rangle,T)$ are plotted in Fig. 5 as a function of $\langle\epsilon\rangle$ for all the temperatures studied. It can be seen that the $k_a(\langle\epsilon\rangle,T)$ initially increases with increasing T (for $T\leqslant500$ K) and subsequently decreases for T above 500 K.

B. Autodetachment frequency $\tau_d^{-1}(\langle\epsilon\rangle,T)$ as a function of $\langle\epsilon\rangle$ and T

As mentioned above, the present measurements and analysis give simultaneously τ_a^{-1} and τ_d^{-1}. The latter was

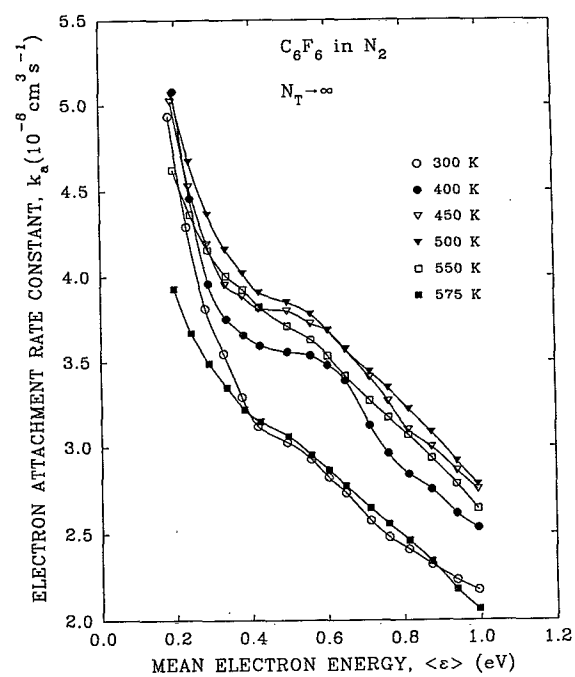

FIG. 5. Electron attachment rate constant k_a (for $N_a\to0$ and $N_T\to\infty$) for C_6F_6 as a function of mean electron energy, $\langle\epsilon\rangle$ at temperatures of 300, 400, 450, 500, 550, and 575 K.

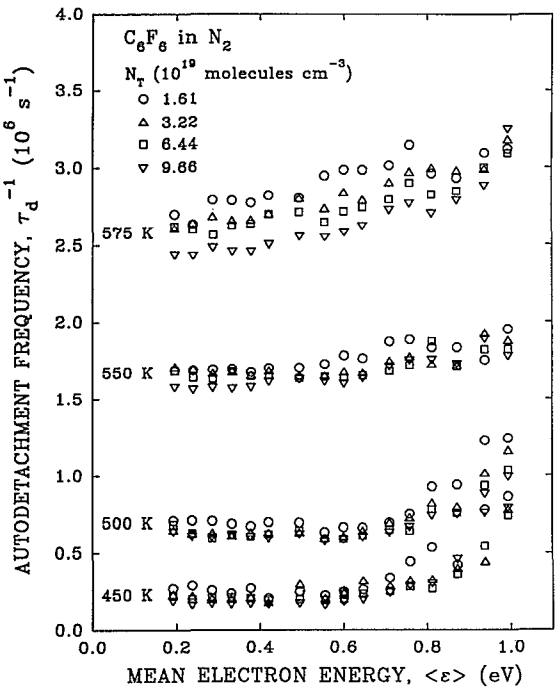

FIG. 6. Autodetachment frequency $\tau_d^{-1}(\langle\epsilon\rangle,T)$ for $C_6F_6^-$ (or $C_6F_6^-$* which were not completely stabilized) as a function of mean electron energy, $\langle\epsilon\rangle$ at 450, 500, 550, and 575 K and the total gas number densities, N_T, of (○) 1.61, (△) 3.22, (□) 6.44, and (▽) 9.66×10^{19} molecules cm^{-3}.

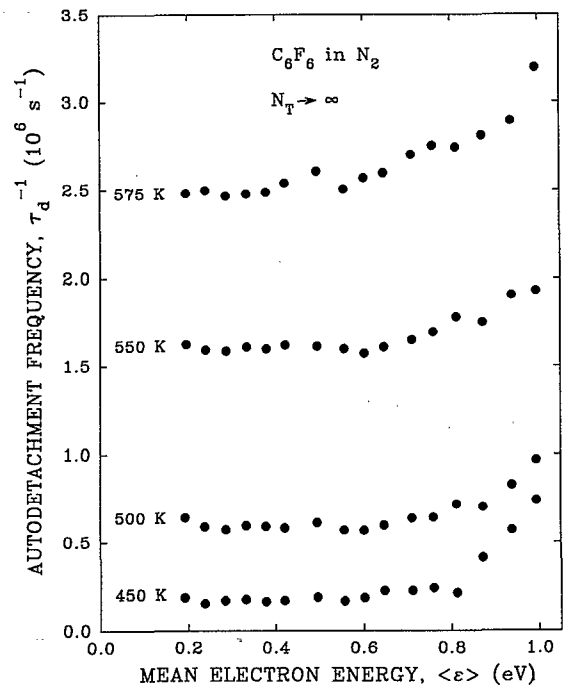

FIG. 7. Autodetachment frequency $\tau_d^{-1}(\langle\epsilon\rangle,T)$ (for $N_T\rightarrow\infty$) for $C_6F_6^-$ as a function of mean electron energy, $\langle\epsilon\rangle$ at 450, 500, 550, and 575 K. (For T below 450 K the τ_d^{-1} was too small to be measured with the present technique.)

determined as a function of $\langle\epsilon\rangle$ for 450, 500, 550, and 575 K. These are plotted in Fig. 6 for total gas number densities $N_T=1.61$, 3.22, 6.44, and 9.66×10^{19} molecules cm^{-3}. It can be seen from Fig. 6 that τ_d^{-1} increases sharply as T is raised from 450 to 575 K and for a fixed $\langle\epsilon\rangle$ and T it becomes smaller the higher the N_T. The increase of τ_d^{-1} with T is due to the increase in the internal energy of $C_6F_6^-$ as T is raised (see later in this section) and the decrease of τ_d^{-1} with N_T is due to the fact that as N_T is increased progressively a larger number of the initially unstable $C_6F_6^-$* become collisionally stabilized. When $N_T\rightarrow\infty$ all $C_6F_6^-$* formed are fully stabilized giving $C_6F_6^-$ thus requiring more energy to revert back to the neutral molecule plus a free electron [reaction (2)]. In order to obtain the value $\lim_{N_T\rightarrow\infty}[\tau_d^{-1}(\langle\epsilon\rangle,T)]$, the $\tau_d^{-1}(\langle\epsilon\rangle,T)$ was determined as a function of the total gas number density N_T (for sufficiently low values of N_T, $C_6F_6^-$* can decay without being fully stabilized), plotted as a function of $1/N_T$ and extrapolated to $1/N_T\rightarrow0$. The values $\tau_d^{-1}(\langle\epsilon\rangle,T)$ obtained this way correspond to the autodetachment frequency for the fully stabilized parent anions $C_6F_6^-$ and are plotted in Fig. 7. Below 450 K the $\tau_d^{-1}(\langle\epsilon\rangle,T)$ (in the $\langle\epsilon\rangle$ range studied) were very small and the uncertainty in their determination large since there is very little autodetachment taking place.

C. Swarm unfolded electron attachment cross section $\sigma_a(\epsilon,T)$

The small number of attaching gas molecules (compared to that for N_2) employed in the present study, is not expected to change the electron energy distribution function $f(\epsilon,\langle\epsilon\rangle,T)$ of N_2 which we can assume to be the same for N_2 and for the C_6F_6/N_2 gas mixtures used in this study. This is also evident from Fig. 3 where $k_a(\langle\epsilon\rangle,T)$ shows no overall dependence on N_a. We can then determine the total electron attachment cross section $\sigma_a(\epsilon,T)$ using an iterative electron swarm-unfolding technique[32] to unfold the total electron attachment rate constants $k_a(\langle\epsilon\rangle,T)$ shown in Fig. 5. The swarm-unfolded $\sigma_a(\epsilon,T)$ are plotted as a function of the incident electron energy ϵ for 300, 400, 450, 500, 550, and 575 K in Fig. 8. They show maxima at ~0.0 and at ~0.8 eV. The positions of the maxima are consistent with earlier studies[5] which found the electron attachment cross section for C_6F_6 at 300 K to possess two peaks, one at thermal energies and another at ~0.73 eV and associated the former peak with electron capture into the π_4 or π_5 orbitals and the latter into the π_6 orbital.

D. Variation of the electron attachment and detachment frequencies in C_6F_6 with, respectively, the internal energy of C_6F_6 and $C_6F_6^-$

Clearly the results of this study show that in the temperature range investigated in this paper, the temperature influences profoundly the autodetachment process [reaction (2)] but it has only a small effect on the electron capture process [reaction (1)]. In the present study the transient $C_6F_6^-$* anion formed initially by the capture of an electron, is stabilized by collisions with N_2 molecules (resulting in $C_6F_6^-$). Some anions obviously undergo autodetachment while still excited. As $N_T\rightarrow\infty$ all of the $C_6F_6^-$* anions become stabilized before autoejecting the electron back into the medium. Assuming that the cross section for

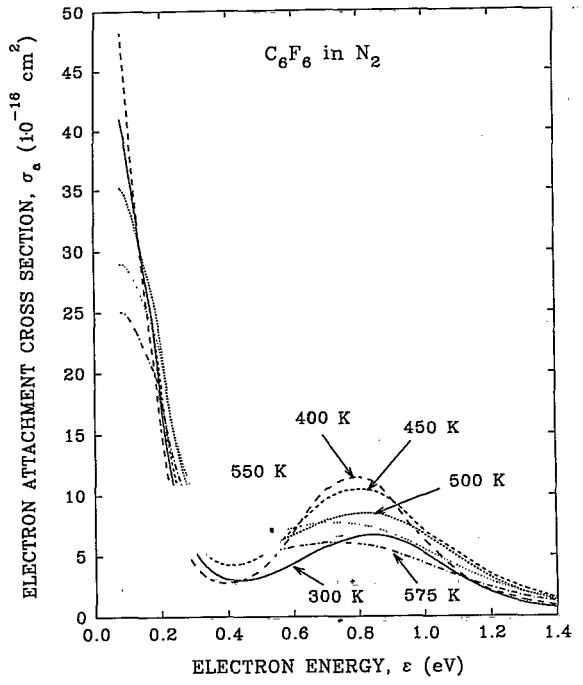

FIG. 8. Swarm unfolded total electron attachment cross sections $\sigma_a(\epsilon,T)$ for C_6F_6 at 300, 400, 450, 500, 550, and 575 K.

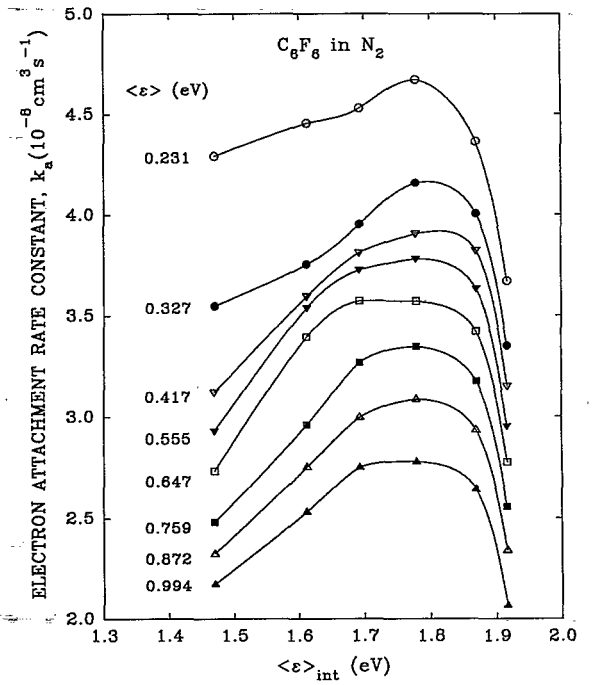

FIG. 9. Electron attachment rate constant, k_a (for $N_T \to \infty$) for $C_6F_6^-$ as a function of $\langle\epsilon\rangle_{int}$ for various values of the mean electron energy.

the collision between $C_6F_6^{-*}$ and N_2 is given by the classical Langevin expression[33] an estimate for the time τ_c between collisions can be determined from

$$\tau_c = \frac{1}{2\pi N_T}\left(\frac{M_r}{e^2\alpha}\right)^{1/2}, \tag{10}$$

where M_r is the reduced mass of the $C_6F_6^-$, N_2 system and α is the static polarizability of N_2 ($=1.7403\times10^{-24}$ cm^3).[34] For the gas number densities N_T employed in this study τ_c varies from $\sim10^{-11}$ to $\sim10^{-10}$ s. That is, the times between collisions of $C_6F_6^{-*}$ and N_2 are much shorter than the autodetachment lifetime of the isolated $C_6F_6^{-*}$ anion (for thermal electron capture this lifetime is ~12 μs) (Refs. 3, 17, and 18).

In an effort to better understand the effect of T on τ_a^{-1} and τ_d^{-1} we estimated at each T employed in the present study the vibrational energy of C_6F_6 in excess of the zero-point energy from

$$\langle\epsilon\rangle_{vib}(T) \approx \sum_{i=1}^{N} \frac{\hbar\omega_i}{e^{\hbar\omega_i/kT}-1} \tag{11}$$

using the vibrational frequencies listed in Refs. 35–37 and assumed that the total internal energy $\langle\epsilon\rangle_{int}(T)$ of both C_6F_6 and $C_6F_6^-$ is given by this quantity. We then plotted the electron attachment rate constant and the autodetachment frequency as a function of $\langle\epsilon\rangle_{int}$ in Figs. 9 and 10, respectively. The $k_a(\langle\epsilon\rangle,\langle\epsilon\rangle_{int})$ first increases and then decreases with $\langle\epsilon\rangle_{int}$ but the changes are small compared to those of $\tau_d^{-1}(\langle\epsilon\rangle,\langle\epsilon\rangle_{int})$. The autodetachment frequency at all values of $\langle\epsilon\rangle$ increases monotonically with increasing internal energy; by more than one order of magnitude (see Fig. 10) when $\langle\epsilon\rangle_{int}$ increases from ~1.69 to ~1.92 eV.

If we assume that the autodetachment process requires an activation energy E^* and that τ_d^{-1} is related to T by

$$\tau_d^{-1} = Ae^{-E^*/kT} \tag{12}$$

then E^* can be estimated from a plot of $\ln(\tau_d^{-1})$ as a function of $1/T$. A plot of this nature is shown in Fig. 11.

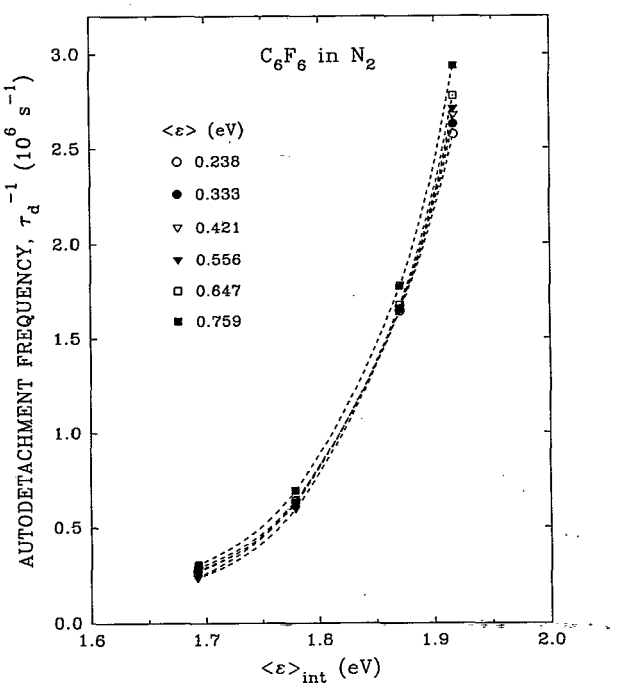

FIG. 10. Autodetachment frequency, τ_d^{-1} (for $N_T \to \infty$) for $C_6F_6^-$ as a function of $\langle\epsilon\rangle_{int}$ for various values of the mean electron energy.

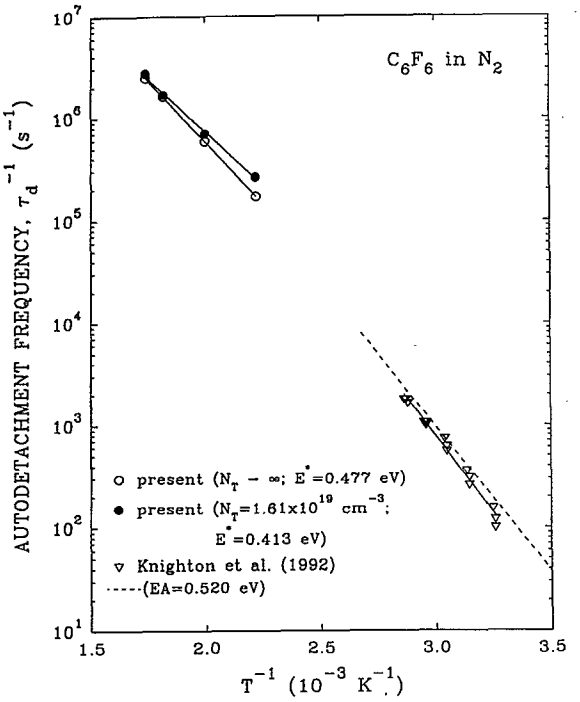

FIG. 11. Autodetachment frequency, τ_d^{-1} (for $\langle\epsilon\rangle \to 3/2kT$) for $C_6F_6^-$ as a function of $1/T$. The open circles are for $N_T \to \infty$ and the closed circles for $N_T = 1.61 \times 10^{19}$ molecules cm^{-3}. Also plotted in the figure are the τ_d^{-1} data of Ref. 25 we extracted from Fig. 9 of that paper. The slope of the solid line through their data corresponds to an E^* of 0.603 eV. The broken line through their data corresponds to an E^* value of 0.52 eV which is the value reported by Ref. 13 for the EA of C_6F_6.

The τ_d^{-1} data plotted in Fig. 11 are for thermal electrons and for two values of N_T (see figure caption). From the slope of $\ln(\tau_d^{-1})$ vs $1/T$ for $N_T \to \infty$ (i.e., completely stabilized $C_6F_6^-$) we estimated E^* to be 0.477 eV. The slope for a similar plot in Fig. 11 for $N_T = 1.61 \times 10^{19}$ molecules cm^{-3} is 0.413 eV indicating that at this N_T not all $C_6F_6^-$ were in their lowest internal energy state. The value for E^* of $N_T \to \infty$ would correspond to the case that all negative ions reach adiabatically the ground electronic state for the neutral, from the lowest possible internal energy state of the anion and should compare well—as apparently it does—with the value for the electron affinity of C_6F_6 (EA=0.52 eV) reported in Ref. 13. Both of these values were basically determined by looking at the autodetachment process; the present one by looking at the autodetached electrons at microsecond and submicrosecond times and that of Ref. 13 at the decline of the negative ion density at ms time scales. The E^* values of the present study and the EA of Refs. 13 and 25 are lower than the EA values reported by other workers [i.e., ~0.86 eV (Ref. 14), >1.8 eV (Ref. 7)]. Also plotted in Fig. 11 are the data for τ_d^{-1} between 300 and 350 K measured in Ref. 25 for thermal electrons, which at 350 K are almost two orders of magnitude lower than our values for τ_d^{-1} for 450 K. Such small τ_d^{-1} would be undetected in our electron current waveforms and the perturbation of such a process in the measurement of k_a would be increasingly negligible for T below 450 K. We fitted the data from Ref. 25 with Eq. (12) and the solid line through their points has a slope which corresponds to an activation energy $E^* = 0.603$ eV. We also plotted our measured values for $\tau_d^{-1}(T)$ at mean electron energies higher than thermal to see possible effects of the captured electron's energy on E^*. The results obtained show that at higher $\langle\epsilon\rangle$ the E^* are somewhat smaller than for $\langle\epsilon\rangle = 3/2kT$. For example, when the mean energy of the electron swarm is 0.759 eV fitting of the $\tau_d^{-1}(T)$ to Eq. (12) yields an activation energy 0.425 eV for $N_T \to \infty$.

Finally, besides the basic significance of the present study the quantitative understanding of the effects of T on the electron attachment and detachment properties of electronegative gases is important in determining the dielectric properties of gaseous dielectrics especially when avalanche initiation is triggered by autodetachment.

ACKNOWLEDGMENTS

Research sponsored by the Wright Laboratory, U.S. Department of the Air Force, under Contract No. AF 33615-92-C-2221 with the University of Tennessee and the Office of Health and Environmental Research, U.S. Department of Energy under Contract No. DE-AC05-84OR21400 with Martin Marietta Energy Systems, Inc.

[1] J. R. Frazier, L. G. Christophorou, J. G. Carter, and H. C. Schweinler, J. Chem. Phys. **69**, 3807 (1978).
[2] V. H. Dibeler, R. M. Reese, and F. L. Mohler, J. Chem. Phys. **26**, 304 (1957).
[3] W. T. Naff, C. D. Cooper, and R. N. Compton, J. Chem. Phys. **49**, 2784 (1968).
[4] T. Oster, A. Kühn, and E. Illenberger, Int. J. Mass Spectrom. and Ion Processes **89**, 1 (1989).
[5] K. S. Gant and L. G. Christophorou, J. Chem. Phys. **65**, 2977 (1976).
[6] F. M. Page and G. C. Goode, *Negative Ions and the Magnetron* (Wiley–Interscience, New York, 1969).
[7] C. Lifschitz, T. O. Tiernan, and B. M. Hughes, J. Chem. Phys. **59**, 3182 (1973).
[8] L. J. Rains, H. W. Moore, and R. J. McIver, J. Chem. Phys. **68**, 3309 (1978).
[9] R. N. McDonald, A. K. Chowdhury, and D. W. Setser, J. Am. Chem. Soc. **103**, 7588 (1981).
[10] U. Sowada and R. A. Holroyd, J. Phys. Chem. **84**, 1150 (1984).
[11] E. C. M. Chen, W. E. Wentworth, and T. J. Limero, J. Chem. Phys. **83**, 6541 (1985).
[12] P. Kebarle and E. P. Grimsrud, J. Phys. Chem. **90**, 2747 (1986).
[13] S. Chowdhury, E. P. Grimsrud, T. Heinis, and P. Kebarle, J. Am. Chem. Soc. **108**, 3630 (1986).
[14] W. E. Wentworth, T. Limero, and E. C. M. Chen, J. Phys. Chem. **91**, 241 (1987).
[15] A. A. Christodoulides, D. L. McCorkle, and L. G. Christophorou, *Electron–Molecule Interactions and Their Applications*, edited by L. G. Christophorou (Academic, Orlando, 1984), Vol. 2, Chap. 6.
[16] P. Smith, J. Chem. Phys. **29**, 681 (1958).
[17] L. G. Christophorou, Adv. Electron. Electron Phys. **46**, 55 (1978).
[18] L. G. Christophorou, K. S. Gant, and V. E. Anderson, J. Chem. Soc. Faraday Trans. II **73**, 804 (1977).
[19] F. J. Davis, R. N. Compton, and D. R. Nelson, J. Chem. Phys. **59**, 2324 (1973).
[20] N. G. Adams, D. Smith, E. Alge, and J. Burdon, Chem. Phys. Lett. **116**, 460 (1985).
[21] N. Hernandez-Gil, W. E. Wentworth, T. Limero, an E. C. M. Chen, J. Chromatogr. **312**, 31 (1984).
[22] E. C. M. Chen, W. E. Wentworth, and T. Limero, J. Chem. Phys. **83**, 6541 (1985).

[23] S. M. Spyrou and L. G. Christophorou, J. Chem. Phys. **82**, 1048 (1985).
[24] L. G. Christophorou, J. Chem. Phys. **83**, 6543 (1985).
[25] W. B. Knighton, J. A. Bognar, and E. P. Grimsrud, Chem. Phys. Lett. **192**, 522 (1992).
[26] L. G. H. Huxley and R. W. Crompton, *The Diffusion and Drift of Electrons in Gases* (Wiley–Interscience, New York, 1974); S. R. Hunter and L. G. Christophorou, *Electron–Molecule Interactions and Their Applications*, edited by L. G. Christophorou (Academic, Orlando, 1984), Vol. 2, Chap. 3.
[27] A. V. Phelps and L. C. Pitchford, Phys. Rev. A **31**, 2932 (1985); S. R. Hunter, J. G. Carter, and L. G. Christophorou, J. Chem. Phys. **90**, 4879 (1989).
[28] L. Frommhold, Fortschr. Phys. **12**, 597 (1964).
[29] C. Wen, Ph.D. dissertation, Eindhoven University of Technology, The Netherlands, 1989.
[30] C. Wen and J. M. Wetzer, IEEE Trans. Electr. Insul. **23**, 999 (1988); **24**, 143 (1989).
[31] T. H. Teich, in *Gaseous Dielectrics VI*, edited by L. G. Christophorou and I. Sauers (Plenum, New York, 1991), pp. 215–229.
[32] L. G. Christophorou, D. L. McCorkle, and V. E. Anderson, J. Phys. B **4**, 1163 (1971).
[33] P. Langevin, Ann. Chim. Phys. **5**, 245 (1905).
[34] R. H. Orcutt and R. H. Cole, J. Chem. Phys. **46**, 697 (1967).
[35] D. Steele and D. H. Whiffen, Trans. Faraday Soc. **55**, 369 (1959).
[36] R. A. R. Pearce, D. Steele, and K. Radcliffe, J. Mol. Struct. **15**, 409 (1973).
[37] F. Török, Á. Hegedűs, K. Kósa, and P. Pulay, J. Mol. Struct. **32**, 98 (1976).